Heriot-Watt University

Heriot-Watt University
Research Gateway

Picosecond Laser Micro-welded Similar and Dissimilar Material

Carter, Richard; Chen, Jianyong; Shephard, Jonathan D; Thomson, Robert R; Hand, Duncan Paul

Publication date:
2014

Link to publication in Heriot-Watt Research Gateway

Citation for published version (APA):
Carter, R., Chen, J., Shephard, J. D., Thomson, R. R., & Hand, D. P. (2014). Picosecond Laser Micro-welded Similar and Dissimilar Material. Paper presented at 15th International Symposium on Laser Precision Microfabrication, Vilnius, Lithuania.

General rights
Copyright and moral rights for the publications made accessible in the public portal are retained by the authors and/or other copyright owners and it is a condition of accessing publications that users recognise and abide by the legal requirements associated with these rights.

If you believe that this document breaches copyright please contact us providing details, and we will remove access to the work immediately and investigate your claim.

Picosecond Laser Micro-welded Similar and Dissimilar Material

Richard M. CARTER[*1], Jianyong CHEN[1], Jonathan D. SHEPHARD[1], Robert R. THOMSON[1] and Duncan P. HAND[1]

[*1]*Institute of Photonics and Quantum Sciences, School of Engineering and Physical Sciences, Heriot Watt University, Edinburgh, EH14 4AS, United Kingdom*
E-mail: R.M.Carter@hw.ac.uk

We report the successful picoseconds laser welding of a range of similar and dissimilar materials. The welds are formed by a tightly focused 1030 nm, 5.9 ps, 400 kHz laser system which induces microplasma formation. With suitably well prepared samples the plasma is confined and re-solidifies into a weld. Due to the speed of the interaction time between laser and material the heat affected zone is restricted to a few 100 µm around the weld making it an essentially cold process. We specifically report the capability to weld fused silica, borosilicate and sapphire to aluminium, copper, stainless steel, silicon and silicon carbide. Analysis of material mobility in fused silica welds has been investigated through confocal fluorescent microscopy of an Nd doped sample welded to an undoped sample. The results indicate limited mobility in the head affected zone but high mobility in the microplasma region. While the process requires significant surface preparation (Ra < 60nm) the versatility of the process allows a wide range of materials to be welded with essentially the same laser system.

Keywords: microwelding, picosecond, ultrafast, laser, material processing

1. Introduction

The joining of small parts forms an integral part of a range of industries [1-3]. A large variety of methods including: adhesive bonding, fusion bonding, arc welding, anodic bonding, soldering, frit and micro-welding have been developed for a range of MEMS, micro-optic, micro-fluidic, silicon chip and sensor devices. Laser micro-welding, in particular, has been the subject of significant study in recent years due to the advantages of small heat affected zones (HAZ), high precision and high speed while simultaneously eliminating the need for an interlayer with the associated issues of out gassing, creep and aging problems. Laser microwelding allows for the essentially cold direct bonding of materials [4-8].

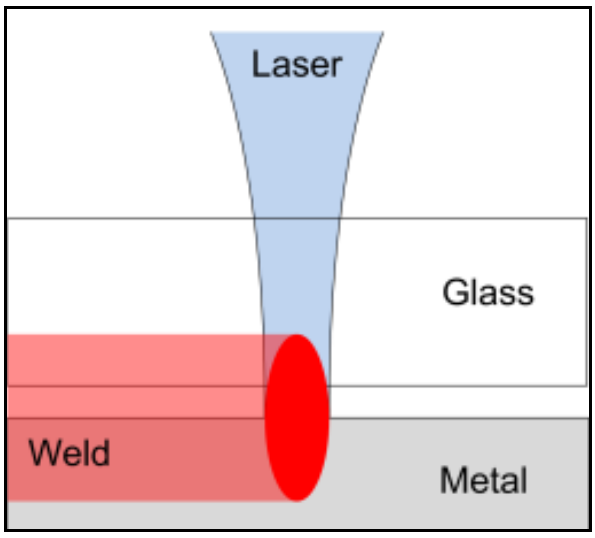

Fig. 1: Illustration of laser microwelding principle

The basic principle of laser micro-welding is to focus a, typically ultrafast, laser beam onto the join between two materials. The incident radiation is absorbed locally melting or forming a microplasma which, once cooled, forms a solid join (Fig. 1).

Laser micro-welding is dependent on the properties of ultra-short pulsed lasers. These ultra-short pulses allow for highly localized absorption within otherwise transparent material through non-linear multiphoton processes. This allows a weld seam to be accurately positioned on the join of two materials without damaging or heating the surrounding bulk material. The heated zone melts or forms a microplasma that expands, fills any gap and solidifies into a solid join [4,5].

The short interaction times between optical radiation and material allows for the direct bonding of highly (thermally) dissimilar material, e.g. glass and metal, as the interactions occur on a significantly shorter timescale than thermal expansion or conduction.

A successful weld is, however, dependant on the effective confinement of the melt or, in particular, microplasma which can only be achieved by a very small gap between the two materials. In general optical contact (< 1 µm) is required to achieve a successful weld [5]. Some materials, e.g. optical glasses, crystals etc. are commercially available with suitable λ/4 flatness as standard other materials, particularly metals, require significant and careful processing to achieve the required surface finish. Care must also be taken to ensure that the materials remain sufficiently clean, a process which is non-trivial outside a cleanroom environment.

The majority of work carried out to date has focused on the use of femtosecond laser systems [4,6,8,9-15]. While these ultra-short pulsed systems allow for extremely high precision it has been recently shown that similar results are

achievable using less expensive picoseconds systems [16-19].

While localized welding is possible using high power single short systems [5] in general it is necessary to use thermal accumulation for fast efficient generation of micro-welds. This requires that individual pulses arrive before the energy of the last pulse can dissipate. For most materials this is on the order of a few microseconds and as a result laser repetition rates of a few hundred kilohertz are required [7].

2. Welding setup

The laser used for our experiments is a Trumpf Tru Micro 5X50. This laser provides 5.9 ps pulses (Fig. 2) centered at 1060 nm at a rate of up to 400 kHz. While the laser is capable of providing average powers of up to 50 W the welding process requires significantly less power (1-2 W) and as such a half wave plate and polarizing beam splitter have been employed as an external variable attenuator, Fig. 3. Ideally the weld geometry would be drawn with a scan head, however sufficiently short focal length scan optics are not generally available and as such a fixed lens has been used with translation provided by stages. The beam is then focused through a plano-convex achromatic lens with a short focal length, typically a numerical aperture of 0.5, giving a small focal spot (1.2 micrometers).

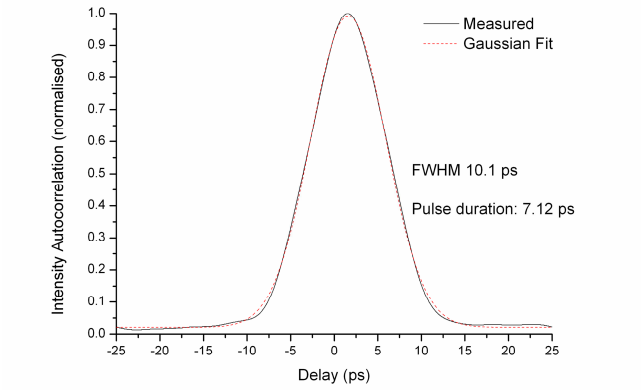

Fig. 2: Autocorrelation of ps pulses used for microwelding.

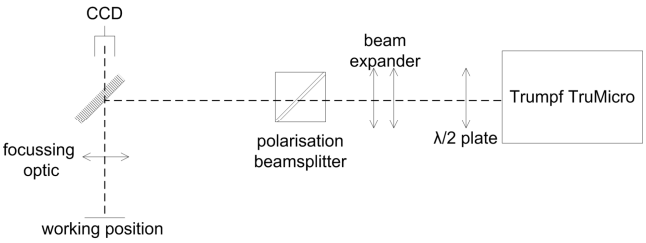

Fig. 3: Schematic of laser train used for microwelding experiments.

To achieve the necessary material gap the two materials are forced together using a pneumatically actuated piston, similar approaches have been widely reported [4,6,5,12]. This piston presses the samples into three equilaterally spaced bearings which forms a four point loading system. The piston is aligned such that an area of optical contact is formed aligned with the incident laser beam. While optical quality glasses can be used with no further surface preparation other than cleaning, metal surfaces require polishing to a mirror (Ra < 60 nm) finish.

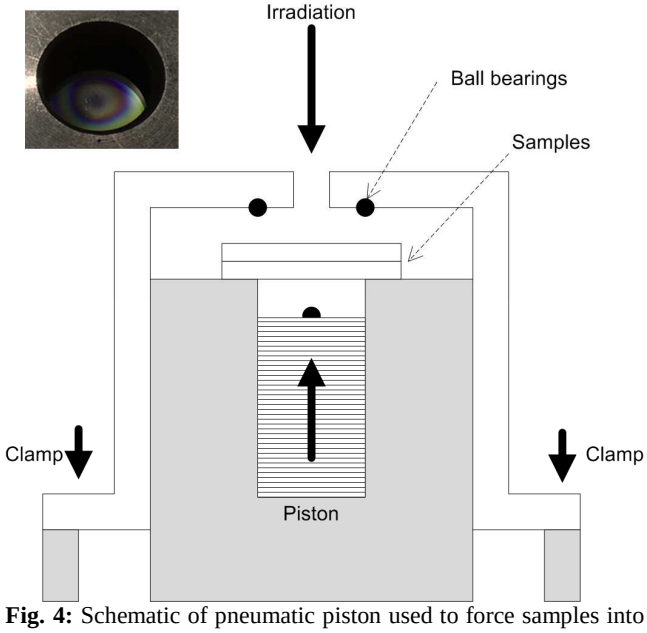

Fig. 4: Schematic of pneumatic piston used to force samples into optical contact. Inset - example photograph of optical contact.

The clamp setup is mounted on a set of Aerotech screw stages which provide three axis translation with an accuracy of approximately six micrometers. The chosen weld pattern is an Archimedean spiral with a pitch of 0.1 mm beginning at 2π and extending to a final radius of 1.25 mm (25π) at a constant velocity of 1 mm s^{-1}, Fig. 5. This spiral pattern was chosen to ensure that the weld seam begins at the position of closest contact and expands without corners, which generate additional stress. This arrangement effectively creates a 2.5 mm diameter spot weld.

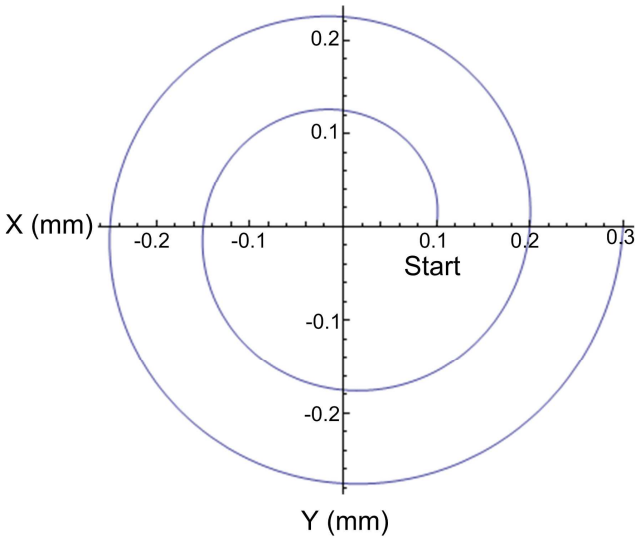

Fig. 5: Illustration of spiral pattern used for welds. Pattern is an Archimedean spiral with pitch of 0.1 mm extending to final radius (not shown) of 1.25 mm.

3. Cross-sectional Analysis

To investigate the mobility of material during the weld process two borosilicate glasses were welded together, one doped with 4% Nd. The Nd doping acts as a fluorescence

marker and can be analyzed through fluorescence microscopy. This sample was then sectioned and polished.

A confocal Raman microscope was used to analyze the Nd concentration across the weld cross-section by pumping at 785 nm and observing the emission. Fig. 6 shows comparative plots of the fluorescence emission of doped and undoped glass. The emission counts 2.5 nm either side of the 878 nm peak were summed to create and index of Nd (counts).

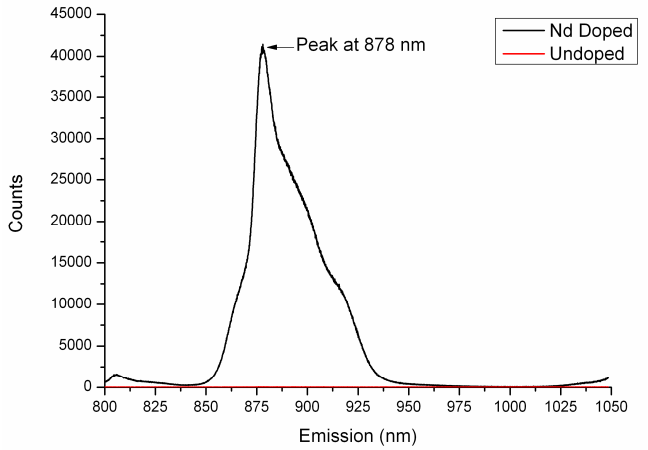

Fig. 6: Plot of emission between 800 and 1050nm of doped (4% Nd) and un-doped borosilicate pumped at 785nm. Note that fluorescence rather than Raman emission dominates.

4. Results

Fig. 7 shows an example weld of SiO_2 - SiO_2. The weld exhibits a characteristic "pulsed" formation modified glass with an inner, highly scattering, plasma zone and an outer HAZ. This formation is characteristic of ultrafast laser, thermal accumulation driven, glass modification [19].

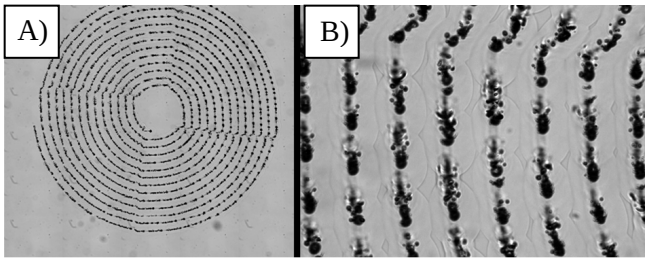

Fig.7: Example microscope images of SiO_2 - SiO_2 weld, a) overview, b) detail [20].

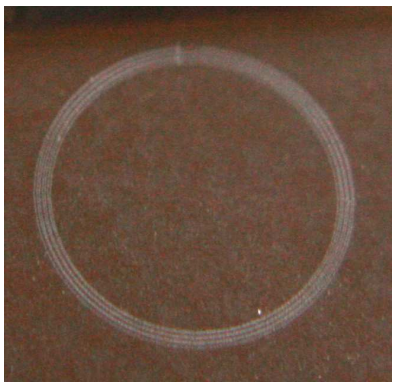

Fig.8: Example of aperture weld in SiO_2 - SiO_2. Inner diameter is 5 mm.

Fracture tests on these welds indicate that both the plasma and HAZ areas are bonded as the break forms around the HAZ. While this forms a strong bond of the order of ~ 600 Nmm^{-2} [20] the inner plasma region of the weld is optically scattering and as a result not appropriate for optical aperture welding. This difficulty can be overcome by welding the perimeter of an aperture. The combination of weld and Van Der Waals act to hold the unwelded central region in optical contact, effectively eliminating the interface [11]. Fig 8 shows an example of this type of weld.

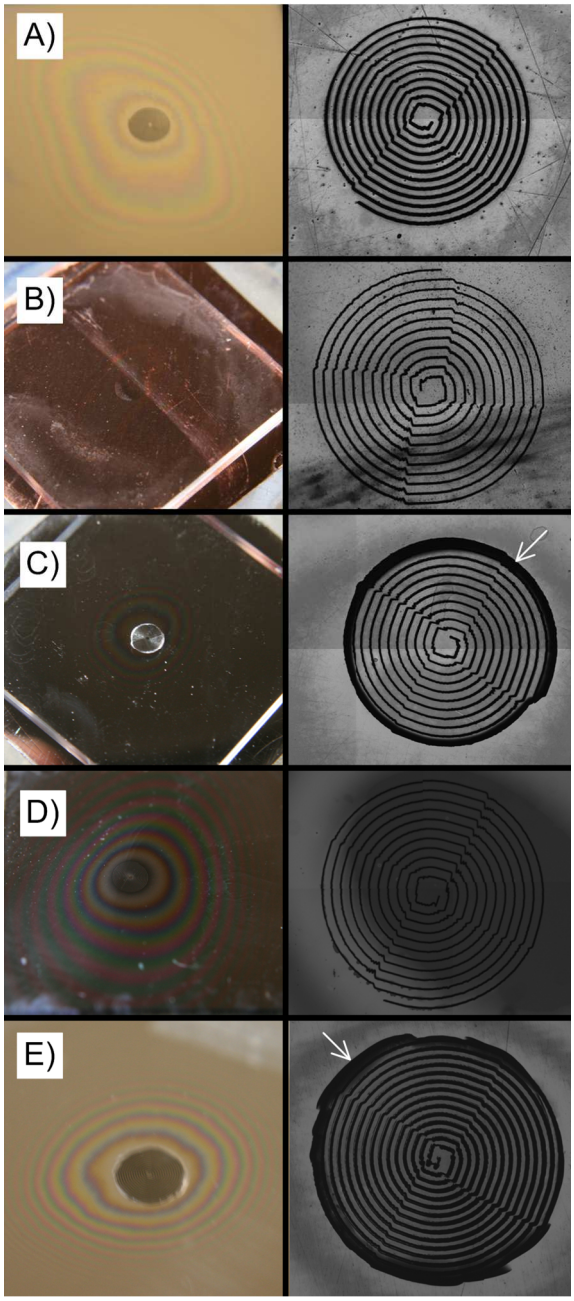

Fig.8: Examples of a) aluminum to SiO_2, b) copper to SiO_2, c) stainless steel (303) to SiO_2, d) silicon to borosilicate and c) sapphire to stainless steel (303). The stainless steel examples exhibit a crack around the weld perimeter (indicated by arrows) which propagates ~ 200 µm into the glass/sapphire [20]

The power required varies depending on material. Fig. 8 illustrates examples of successful welding of aluminum

to SiO_2 and stainless steel to SiO_2. To date aluminum, copper, stainless steel, silicon and silicon carbide have been demonstrated to weld to SiO_2, borosilicate and sapphire at average powers between 1.15 and 2.35 W [20]. In the case of metal welds a continuous seam is formed without the thermal pulsing visible in the SiO_2 - SiO_2 examples. The weld its self is scattering, and therefore appear dark in bright field microscopy.

It is interesting to note that the stainless steel example exhibit a crack around the weld perimeter. This is consistently seen when welding to stainless steel with SiO_2, borosilicate and sapphire but not seen when welding to copper, silicon or aluminum. While the thermal expansion coefficient of stainless steel is low (for a metal) it also has a very low thermal conductivity (for a metal).

It is this low thermal conductivity which gives rise to the cracking. During the weld process (a few minutes) a thermal gradient is established around the weld perimeter. In stainless steel this thermal gradient is very steep due to the low conductivity. Once the weld cools this thermal gradient translates to a stress gradient through thermal expansion and the perimeter cracks. It is worth noting that the cracks here propagate only 200 µm into the glass before self termination. The crack therefore does not prevent the welding of the two materials but likely effects the weld strength.

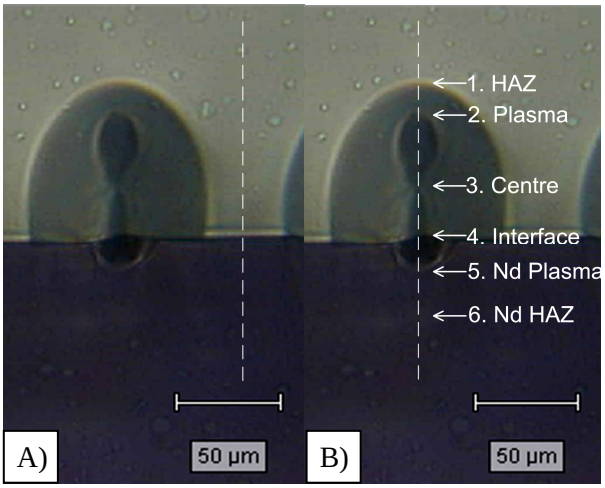

Fig. 9: Cross-sectional microscope images of Nd (4%) doped borosilicate welded to undoped borosilicate. The dotted lines indicate the locations of fluorescence spectroscopy scans in Fig 10. a) clear image with reference un-welded fluorescence scan, b) weld section fluorescence scan with labels indicating points of interest within the weld structure.

Fig. 9 shows the cross-section of the Nd doped fused silica to undoped borosilicate weld. This tear drop or hourglass shaped weld is typical of ultrafast laser modification in glass. The outer region consists of modified glass i.e. the HAZ while the inner region consists of scattering centers consistent with microplasma formation. Two fluorescence sections were taken across this image represented by the dotted lines in Fig. 9a – a reference section over an unwelded region - and b – welded region.

Fig. 10 shows the results of the Raman microscope confocal fluorescence spectroscopy. Fig. 10a shows the control cross-section while Fig. 10b shows the welded region. The numbered points indicate the features of interest labeled in Fig. 9 b). From the Nd count in the reference section we can see the clear dividing line between doped and undoped glass. Since the interface is expected to be abrupt the slope of the plot suggests a resolution of the order of 10 µm, which is consistent with the laser spot used for the fluorescence scan.

The weld section (Fig 10.b) gives some interesting information on the mobility of the glass during the welding process. The HAZ in particular shows limited to zero mobility since there is little to no difference between the counts in this region to the un-welded regions. The plasma zone, (hourglass feature in Fig. 9) shows considerably more mobility but in this case the Nd increases as the trace approaches the interface. There is also a significant difference between the upper and lower lobes of the plasma region; the upper region has less Nd. This indicates that the plasma region is not a true mix of material. Essentially while there is a considerable amount of local intermixing in the plasma region the weld re-solidifies before the material can become homogeneous.

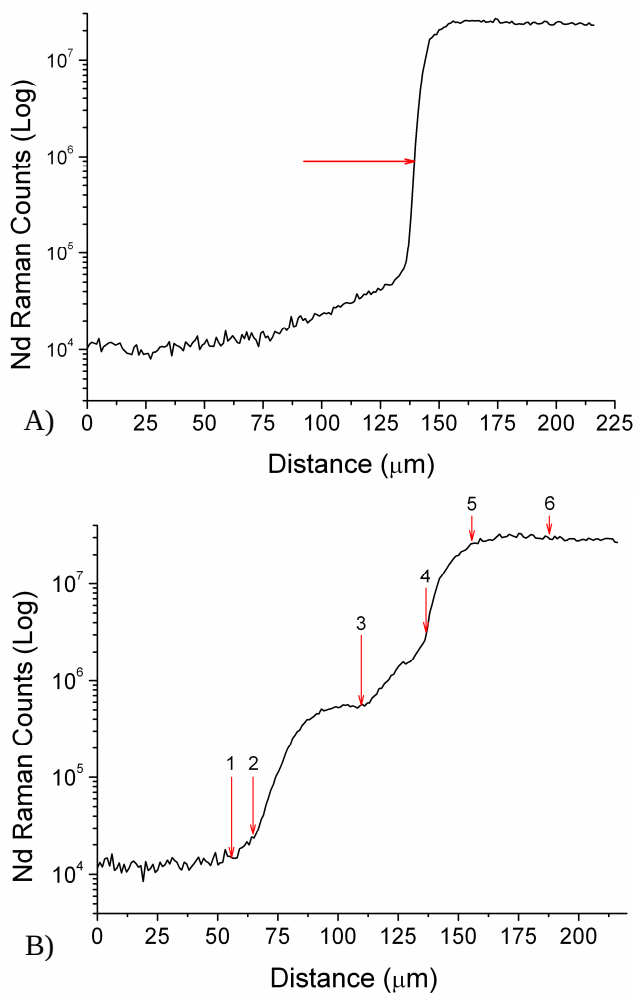

Fig. 10: Plots of fluorescence spectroscopy scans of sectioned Nd doped to undoped borosilicate welds along paths indicated in Fig. 9b. a) Reference scan with no weld, red arrow indicate positon of interface between materials. b) Section across weld centre, arrows indicate position of points of interest from Fig. 9 b).

5. Conclusions

Laser micro-welding with ps pulses has been demonstrated to be capable of welding a wide range of both simi-

lar and dissimilar materials. While careful surface preparation and optical contact are critical in obtaining a successful weld the range of materials which can be directly bonded with essentially the same laser parameters shows significant versatility.

The degree of material intermixing within the weld structure has also been investigated for the first time. The results demonstrate that while the outer HAZ region does not exhibit significant intermixing the inner microplasma region is a true, although inhomogeneous mixture of the materials.

Future work should concentrate on reducing the material preparation requirements by investigating the impact of material roughness and gap size on weld formation.

Acknowledgments

This research was supported by the EPSRC (EP/F02553X/1 and EP/K030884/1) and by Renishaw Plc.

References

[1] F. Niklaus, G. Stemme, J.-Q. Lu, and R. J. Gutmann, *"Adhesive wafer bonding,"* J. Appl. Phys. **99**(3), 031101 (2006).

[2] J. Oberhammer, F. Niklaus, and G. Stemme, *"Sealing of adhesive bonded devices on wafer level,"* Sen. Actuators A **110**(1), 407-412 (2004)

[3] A. W. Y. Tan, and F. E. H. Tay, *"Localized laser assisted eutectic bonding of quartz and silicon by Nd:YAG pulsed-laser,"* Sen. Actuators A, **120**(2), 550-561 (2005).

[4] H. Huang, L.-M. Yang, and J. Liu, *"Ultrashort pulsed fiber laser welding and sealing of transparent materials,"* Appl. Opt. **51**(15), 2979-2986 (2012).

[5] W. Watanabe, T. Tamaki, and K. Itoh, "*Ultrashort Laser Welding and Joining*," in *Femtosecond Laser Micromachining*, O. Roberto, C. Giulio and R, Roberta eds. (Springer-Verlag, 2012) pp 467-477.

[6] Y. Ozeki, T. Inoue, T. Tamaki, H. Yamaguchi, S. Onda, W. Watanabe, T. Sano, S. Nishiuchi, A. Hirose, and K. Itoh, *"Direct welding between copper and glass substrates with femtosecond laser pulses,"* Appl. Phys. Express **1**(8), 82601 (2008).

[7] S. Richter, S. Döring, F. Zimmermann, L. Lescieux, R. Eberhardt, S. Nolte, and A. Tünnermann, *"Welding of transparent materials with ultrashort laser pulses."* Proc. SPIE **8244**, 824402.

[8] W. Watanabe, S. Onda, T. Tamaki, K. Itoh, and J. Nishii, *"Space-selective laser joining of dissimilar transparent materials using femtosecond laser pulses,"* Appl. Phys. Lett. **89**(2), 021106 (2006).

[9] P. Kongsuwan, G. Satoh, and Y. L. Yao, *"Transmission Welding of Glass by Femtosecond Laser: Mechanism and Fracture Strength,"* J. Manuf. Sci. Eng. **134**(1), 011004 (2012).

[10] T. Tamaki, W. Watanabe, and K. Itoh, *"Laser microwelding of transparent materials by a localized heat accumulation effect using a femtosecond fiber laser at 1558 nm,"* Opt. Express **14(**22), 10460-10468 (2006).

[11] D. Hélie, M. Bégin, F. Lacroix, and R. Vallée *"Reinforced direct bonding of optical materials by femtosecond laser welding,"* Appl. Opt. **51**(12), 2098-2106 (2012).

[12] T. Tamaki, W. Watanabe, J. Nishii, and K. Itoh, *"Welding of transparent materials using femtosecond laser pulses,"* Jpn. J. Appl. Phys. **44**, L687-L689 (2005).

[13] A. Horn, I. Mingareev, A. Werth, M. Kachel, and U. Brenk, *"Investigations on ultrafast welding of glass–glass and glass–silicon,"* Appl. Phys. **93**(1), 171-175 (2008).

[14] S. Richter, S. Döring, A. Tünnermann, and S. Nolte, *"Bonding of glass with femtosecond laser pulses at high repetition rates,"* Appl. Phys. **103**(2), 257-261 (2011).

[15] K. Sugioka, M. Iida, H. Takai, and K. Micorikawa, *"Efficient microwelding of glass substrates by ultrafast laser irradiation using a double-pulse train,"* Opt. Lett. **36**(14), 2734-2736 (2011).

[16] I. Miyamoto, A. Horn, and J. Gottmann, *"Local melting of glass material and its application to direct fusion welding by ps-laser pulses,"* J. Laser Micro Nanoen. **2**(1), 7-14 (2007).

[17] I. Alexeev, K. Cvecek, C. Schmidt, I. Miyamoto, T. Frick, and M. Schmidt, *"Characterization of Shear Strength and Bonding Energy of Laser Produced Welding Seams in Glass,"* J. Laser Micro Nanoen. **7**(3), 279-283 (2012).

[18] I. Miyamoto, K. Cvecek, Y. Okamoto, and M. Schmidt, *"Novel fusion welding technology of glass using ultrashort pulse lasers,"* Physics Procedia, **5**(A), 483-493 (2010).

[19] I. Miyamoto, K. Cvecek, and M. Schmidt, *"Evaluation of nonlinear absorptivity in internal modification of bulk glass by ultrashort laser pulses,"* Opt. Express **19**(11), 10714-10727 (2011).

[20] R.M. Carter, J. Chen, J.D. Shephard, R.R. Thomson, and D.P. Hand, *"Picosecond Laser Welding of Similar and Dissimilar Materials,"* App. Opt. accepted for publication and in press (2014)